Turkish Journal of Earth Sciences

Volume 23 | Number 4 Article 3

1-1-2014

Testing of the recently developed tectonomagmatic discrimination diagrams from hydrothermally altered igneous rocks of 7 geothermal fields

KAILASA PANDARINATH

Follow this and additional works at: https://journals.tubitak.gov.tr/earth

 Part of the Earth Sciences Commons

Recommended Citation

PANDARINATH, KAILASA (2014) "Testing of the recently developed tectonomagmatic discrimination diagrams from hydrothermally altered igneous rocks of 7 geothermal fields," *Turkish Journal of Earth Sciences*: Vol. 23: No. 4, Article 3. https://doi.org/10.3906/yer-1401-27
Available at: https://journals.tubitak.gov.tr/earth/vol23/iss4/3

This Article is brought to you for free and open access by TÜBİTAK Academic Journals. It has been accepted for inclusion in Turkish Journal of Earth Sciences by an authorized editor of TÜBİTAK Academic Journals. For more information, please contact academic.publications@tubitak.gov.tr.

TÜBİTAK

Turkish Journal of Earth Sciences

http://journals.tubitak.gov.tr/earth/

Research Article

Turkish J Earth Sci
(2014) 23: 412-426
© TÜBİTAK
doi:10.3906/yer-1401-27

Testing of the recently developed tectonomagmatic discrimination diagrams from hydrothermally altered igneous rocks of 7 geothermal fields

Kailasa PANDARINATH*

Department of Energy Systems, Institute of Renewable Energy, National Autonomous University of Mexico, Temixco, Morelos, Mexico

Received: 20.01.2014 • **Accepted:** 21.04.2014 • **Published Online:** 17.06.2014 • **Printed:** 16.07.2014

Abstract: Recently developed multidimensional tectonomagmatic discrimination diagrams based on log-ratio variables of chemical elements, discordant outlier-free databases, and probability-based boundaries have been shown to work better than the earlier diagrams. Hydrothermally altered drilled well rock cuttings obtained from different depths of geothermal fields were used to test these diagrams to compare the inferred tectonic setting with the expected one. In spite of the hydrothermal alteration effects, these diagrams provided the following expected tectonic settings: (1) an arc setting for Ahuachapán and Berlin geothermal fields, El Salvador; (2) a rift setting for Cerro Prieto geothermal field, Mexico, and Tendaho geothermal field, Afar region; (3) a MORB setting for Reykjanes geothermal field, Iceland; (4) a transitional arc and collision setting for Roman volcanic provenance, Italy; and (5) an arc setting for Tongonan geothermal field, Philippines. The present study indicates that the recently developed multielement discriminant function based diagrams may be successfully applied to infer the original tectonic setting of hydrothermally altered rock samples and thus confirms the robustness of these diagrams.

Key words: Discrimination diagrams, geochemistry, igneous rocks, tectonic setting, arc, rifting, collision

1. Introduction

Tectonomagmatic discrimination diagrams are widely used to infer the original tectonic setting of volcanic rocks with the basic assumption that the characteristic chemical elements of the rocks used in these diagrams are relatively immobile from the period of rock formation to the present. These diagrams are of bivariate (Pearce and Gale, 1977; Pearce and Norry, 1979; Pearce, 1982; Shervais, 1982; Vasconcelos-F. et al., 1998, 2001), ternary (Pearce and Cann, 1973; Pearce et al., 1977; Wood, 1980; Mullen, 1983; Meschede, 1986; Cabanis and Lecolle, 1989), and discriminant function based on element concentrations (Pearce, 1976; Butler and Woronow, 1986; Agrawal et al., 2004). However, the newer multidimensional discriminant function diagrams based on log-transformed ratios (Verma et al., 2006; Agrawal et al., 2008; Verma and Agrawal, 2011; Verma et al., 2012; Verma and Verma, 2013b; Verma et al., 2013) only require that ratios of chemical elements (and not the actual concentrations) remain practically constant.

Although there have been extensive evaluations of these existing diagrams indicating highly variable success rates in inferring the original tectonic setting of the region that the studied rocks represent (Verma et al., 2006, 2010, 2011, 2012; Sheth, 2008; Verma, 2010, 2013; Verma and Verma, 2013a; Pandarinath and Verma, 2013; Verma and Oliveira, 2013), hydrothermally altered rocks have been used less for such evaluations.

Interaction of hydrothermal fluids with surface or subsurface rocks results in changes in their mineralogy and chemical composition (Nicholson, 1993). These changes include the mobility of chemical elements from the solid to liquid or liquid to solid phase, or both. The extent of mobility of the elements depends on various parameters, including degree of hydrothermal alteration, porosity and permeability of rocks etc. Studies on hydrothermal alteration effects in geochemical parameters of volcanic rocks have indicated that some elements are mobile (for example, Si, Mg, Ca, Na, K, Li, Mn, Rb, Sr, Sb, Cs, Ba, and U in rhyolitic rocks in the Yellowstone drill cores (Sturchio et al., 1986); REE in basaltic rock fragments (Palacios et al., 1986), in rhyolitic volcanic rocks (De Groot and Baker, 1992), and in andesitic rocks (Kuschel and Smith, 1992); MnO, P_2O_5, Ta, Zr, and Nb in rhyolitic rock-cuttings of Los Azufres geothermal wells (Pandarinath et al., 2008)) and some other elements are immobile (for example, Ti in obsidian (Dickin, 1981); Zr in oceanic basalts (Humphris and Thompson, 1978; and Zr and Ti in rocks associated with volcanogenic submarine ore deposits (Finlow-Bates

* Correspondence: pk@ier.unam.mx

and Stumpfl, 1981); Ti, Al, Fe, Sc, Co, Y, Zr, REE, Hf, Ta, and Th in rhyolitic rocks in the Yellowstone drill cores (Sturchio et al., 1986); and REE in rhyolitic rock-cuttings of Los Azufres geothermal wells (Pandarinath et al., 2008)). However, Zr and other immobile elements such as Ti can be highly mobile during hydrothermal alteration (for example, Zr in peralkaline rhyolites (Rubin et al., 1993), Zr in rhyolite rocks of Los Azufres geothermal wells (Pandarinath et al., 2008), and Zr and Ti in volcanic rocks (Kelepertsis and Esson, 1987; Verma et al., 2005)).

One of the basic requirements for the reliable application of the older discrimination diagrams to infer the tectonomagmatic origin of the volcanic rocks is that the characteristic chemical elements, which are used in the diagrams, of the rocks are immobile from the period of rock formation to the present. Based on this assumption, several tectonomagmatic discrimination diagrams are developed to infer the original tectonic setting of volcanic rocks (for example, Zr (Pearce and Cann, 1973; Floyd and Winchester, 1975) etc.). Recently, some studies have examined the application of some of the recently developed diagrams to altered rocks. Sheth (2008) evaluated some of the diagrams of Verma et al. (2006) and Vermeesch (2006) with data of ocean-island, arc, and mid-ocean ridge lavas from the Indian Ocean and reported that the log-ratio transformation and linear discriminant analysis appear to be powerful methods in tectonomagmatic discrimination studies. The classification tree-based discrimination of Vermeesch (2006) has already been criticized by Agrawal and Verma (2007). Recently, Pandarinath and Verma (2013) evaluated the more recent and highly successful multielement discriminant function diagrams based on only element concentrations (Agrawal et al., 2004) and on log-transformed ratios (Verma et al., 2006; Agrawal et al., 2008; Verma and Agrawal, 2011) with an application to the basic rocks of on-land and off-shore of northwest Mexico. They observed that these discrimination diagrams have successfully discriminated the original tectonic setting of younger and older on-shore rocks as well as sea-water altered deep-sea rocks and dredged material. Similarly, Verma (2013) successfully evaluated these multidimensional diagrams to infer an ocean island setting for the Hawaiian rocks and a transitional mid-ocean ridge to ocean island setting for the Icelandic rocks.

The postformation changes in the chemical composition of the hydrothermal altered rocks may influence the reliable applicability of these tectnomagmatic discrimination diagrams. Therefore, it is necessary to identify the extent hydrothermal alteration influenced changes in chemical composition of the rocks affect the reliable application of these discrimination diagrams to infer their tectonomagmatic origin. Consequently, in the present study, an attempt is made to determine the robustness of the recently developed and highly successful multielement discriminant function-based tectonomagmatic discrimination diagrams for identifying the original tectonic setting of hydrothermally altered rocks. For this purpose, I have selected the more recent highly successful multielement discriminant function-based diagrams for basic (Verma et al., 2006; Agrawal et al., 2008; Verma and Agrawal, 2011), intermediate (Verma and Verma, 2013b), and acid rocks (Verma et al., 2013) and applied them for inferring the original tectonic setting of the origin of the volcanic rocks in the drilled wells of the geothermal fields. The earlier discrimination function-based diagrams by Agrawal et al. (2004) were also included in this evaluation, because although these diagrams use only adjusted major element concentrations (not element ratios), they were proposed from an extensive database, which is not the case for the older discriminant function diagrams such as those by Pearce (1976) and Butler and Woronow (1986).

2. Studied geothermal fields

Based on the availability of chemical compositional data in the literature for hydrothermally altered rocks, 7 important geothermal fields representing different regions of the world were selected for this study. The volcanic rock samples considered in this study are hydrothermally altered rock cuttings from different depths in the drilled wells of these geothermal fields. There are only limited numbers of geothermal systems, in the literature, which contained the geochemical composition of the altered rocks from the drilled wells. The selected geothermal fields are: (1) Ahuachapán Geothermal Field, El Salvador (3 geothermal wells (Agostini et al., 2006)); (2) Berlin Geothermal Field, El Salvador (5 geothermal wells and 1 lava flow (Agostini et al., 2006; Ruggieri et al., 2006)); (3) Cerro Prieto geothermal field, Mexico (2 geothermal wells; (Herzig, 1990)); (4) Reykjanes geothermal field, Iceland (1 geothermal well (Marks et al., 2010)); (5) Roman Volcanic Province, Italy (4 geothermal wells (Beccaluva et al., 1991)); (6) Tendaho geothermal field, Ethiopia (3 geothermal wells (Gianelli et al., 1998)); (7) Tongonan geothermal field, Philippines (8 geothermal wells (Scott, 2004)). Among these geothermal systems, only the Ahuachapán, Reykjanes, and Roman Volcanic Province geothermal fields contained complete geochemical data (major and trace elements) and the remaining 4 fields have only the major element data for the drilled well rocks. The details regarding the number of geothermal wells, the total number of rock samples along with the corresponding depths in each well, and the available chemical composition data are presented in Table 1.

3. Data analysis procedure

Rock types were determined using the computer program SINCLAS (Verma et al., 2002, 2003). A total of 116 rock

Table 1. Details regarding the hydrothermally altered rock samples obtained from the wells of each geothermal field. Rock type classification is based on SINCLAS computer program of Verma et al. (2002).

Geothermal field	Geothermal well	Total no. of samples	Sample depth (m)	Available geochemical data	Classification of rock types		
					Basic and ultrabasic	Intermediate	Acid
Ahuachapán, El Salvador	AH-34	2	n.a.	Major and trace			
	AH-8	1	n.a.		-	10	4
	TO	11	40–1500				
Berlin, El Salvador	TR-2	6	1450–1650	Major			
	TR-5B	1	n.a.				
	TR-8A	1	1779		4	8	-
	TR-17	2	2000–2417				
	TR-18	1	1053				
	Lava flow	1	-				
Cerro Prieto, Mexico	M-203	10		Major	-	8	6
	M-205	4	3327–3969				
Reykjanes, Iceland	RN-17	50	350–3050	Major and trace	48	2	-
Roman Volcanic	P-2	1	1800	Major and trace			
Province, Italy	P-3	1	297		-	4	-
	CV-2	1	1440				
	CV-3	1	1889				
Tendaho, Ethiopia	TD-1	4	1270–2015	Major			
	TD-2	3	798–1200		11	1	-
	TD-3	5	643–1986				
Tongonan, Philippines	102	1	960	Major			
	202	1	294				
	213	1	147				
	401	2	46–1245		6	4	-
	407	2	760–1070				
	410	1	1822				
	503	1	662				
	MN1	1	309				

n.a.: not available

samples obtained from 26 geothermal wells representing 7 geothermal fields around the world are classified as follows: (1) 64 are of basic and 5 are of ultrabasic type; (2) 37 rocks are of intermediate; and (3) 10 are acid rocks (Table 1). The normal distribution of the variables was achieved by identification and elimination of outlier data points (Barnett and Lewis, 1994) from the software DODESSYS (Verma and Díaz-González, 2012), which allows the application of the multiple-test method initially proposed by Verma (1997) and uses new precise and accurate critical values for discordancy tests (Verma and Quiroz-Ruiz, 2006a, 2006b, 2008, 2010; Verma et al., 2008).

The computer program TecD (Verma and Rivera-Gómez, 2013) was applied for actual counting of samples plotted in different tectonic fields in 20 multidimensional diagrams for basic and ultrabasic magmas (Agrawal et al., 2004, 2008; Verma et al., 2006; Verma and Agrawal 2011), whereas a Statistica spreadsheet was used for probability calculations for intermediate and acid rock samples (Verma and Verma 2013b; Verma et al., 2013). Fifteen new

multidimensional diagrams (3 sets of 5 diagrams for each set) based on complete major elements, combination of immobile major and trace elements, and immobile trace elements developed by Verma and Verma (2013) for intermediate and Verma et al. (2013b) for acid rocks are applied in this work.

4. Results and discussion

Rock type classification indicated that: (1) basic-ultrabasic rocks are available only for the Berlin, Reykjanes, Tendajo, and Tongonan geothermal fields; (2) intermediate rock type is available for all 7 studied geothermal fields; and (3) acid rock type is available only for the Ahuachapán and Cerro Prieto geothermal fields (Table 1). The compiled geochemical database consists of only major element data for the Ahuachapán, Berlin, Cerro Prieto, Reykjanes, Tendajo, and Tongonan geothermal fields, whereas combined major and trace element data are available for the Ahuachapán, Reykjanes, and Roman Volcanic Province geothermal fields (Table 1). The geochemical data of the hydrothermally altered well rocks for each geothermal field were used for applying the corresponding discrimination diagrams of basic-ultrabasic, intermediate, and acid rocks, depending on the available rock type. Rock samples representing different tectonic fields in the diagrams were identified and their percentages (wherever samples number more than 10) were calculated. The discrimination diagrams (Figures 1–3) and the tables showing the percentage of rocks representing the each tectonic setting are presented for only basic-ultrabasic rocks (Tables 2–4). To limit the number of figures, numbers of samples plotted in each tectonic setting (IA = Island Arc; CA = Continental Arc; CR = Continental Rift; OI = Ocean Island, and Col = Collision) are identified based on their probability calculations, counted, percentages are calculated (wherever samples number more than 10), and are summarized in Table 5 for intermediate rocks and in Table 6 for acid rocks.

4.1. Ahuachapán geothermal field, El Salvador

The compiled database consists of major element and trace element data for 14 hydrothermally altered rock samples (10 intermediate and 4 acid rocks) representing different depths in 3 wells of the Ahuachapán geothermal field (Table 1). In probability calculations of the set of 5 new multidimensional tectonomagmatic discrimination diagrams based on major element composition data for intermediate rocks (Verma and Verma, 2013b), the first diagram (with the tectonic setting fields of IA+CA, CR+OI, Col; Table 5) indicated 7 out of 10 samples in the combined field of IA+CA. The second (8 out of 10), third (7 out of 10), and fourth diagrams (6 out of 10) indicated a dominant IA tectonic setting (Table 5). The fifth diagram (with the tectonic setting fields of CA, CR+OI, Col), from which the IA setting is missing, can be considered inapplicable. This shows that the major elements-based diagrams of Verma and Verma (2013b) for intermediate rocks have consistently indicated an IA setting. Similarly, in the probability calculations of the set of 5 diagrams based on immobile major and trace elements (Verma and Verma, 2013b), the first diagram (with the tectonic setting fields of IA+CA, CR+OI, Col; Table 5) indicated that all 8 samples plotted in the combined field of IA+CA, whereas all 8 samples plotted in IA tectonic setting field in the second, third, and fourth diagrams. The fifth diagram (with the tectonic setting fields of CA, CR+OI, Col), from which IA setting is missing, can be considered inapplicable. This indicates that, similar to the major elements-based diagrams, the set of immobile major and trace elements-based diagrams of Verma and Verma (2013b) have also consistently indicated an IA setting for these intermediate rocks.

Similarly, the major elements-based diagrams for acid rocks (Verma et al., 2013) have indicated a dominant IA setting, whereas the diagrams based on combination of immobile major and trace element for acid rocks (Verma at al., 2013) have suggested a dominant CA setting (Table 6).

The expected tectonic setting for the rocks of these geothermal wells is continental arc. Geochemical differentiation between island and continental arc settings is difficult. Therefore, it may be considered that these diagrams have indicated a general arc setting.

4.2. Berlin geothermal field, El Salvador

The compiled database consists of only major element data for 12 hydrothermally altered rock samples (3 basic, 1 ultrabasic, and 8 acid rocks) representing 5 wells of the Berlin geothermal field (Table 1). The set of 5 major element-based (Agrawal et al., 2004; Figure 1) and the set of 5 major element log-ratios-based (Verma et al., 2006; Figure 2) discrimination diagrams for the basic-ultrabasic rocks have suggested an IA setting for these rocks (Tables 2 and 3). The arc setting in each set of these diagrams is represented by island arc only and there is no continental tectonic setting field is present in these diagrams. Hence, it may be considered a general arc setting for these rocks.

The major elements-based diagrams for intermediate rocks (Verma and Verma, 2013b) have suggested a dominant CA setting for the altered rocks of the wells of this geothermal field (Table 5).

The inferred CA tectonic setting for the rocks of these geothermal wells is consistent with the known tectonic setting for this geothermal field.

4.3. Cerro Prieto geothermal field, Mexico

The compiled database consists of only major element data for 14 hydrothermally altered rock samples (8 intermediate and 6 acid rocks) representing different depths in 5 wells of the Cerro Prieto geothermal field (Table 1).

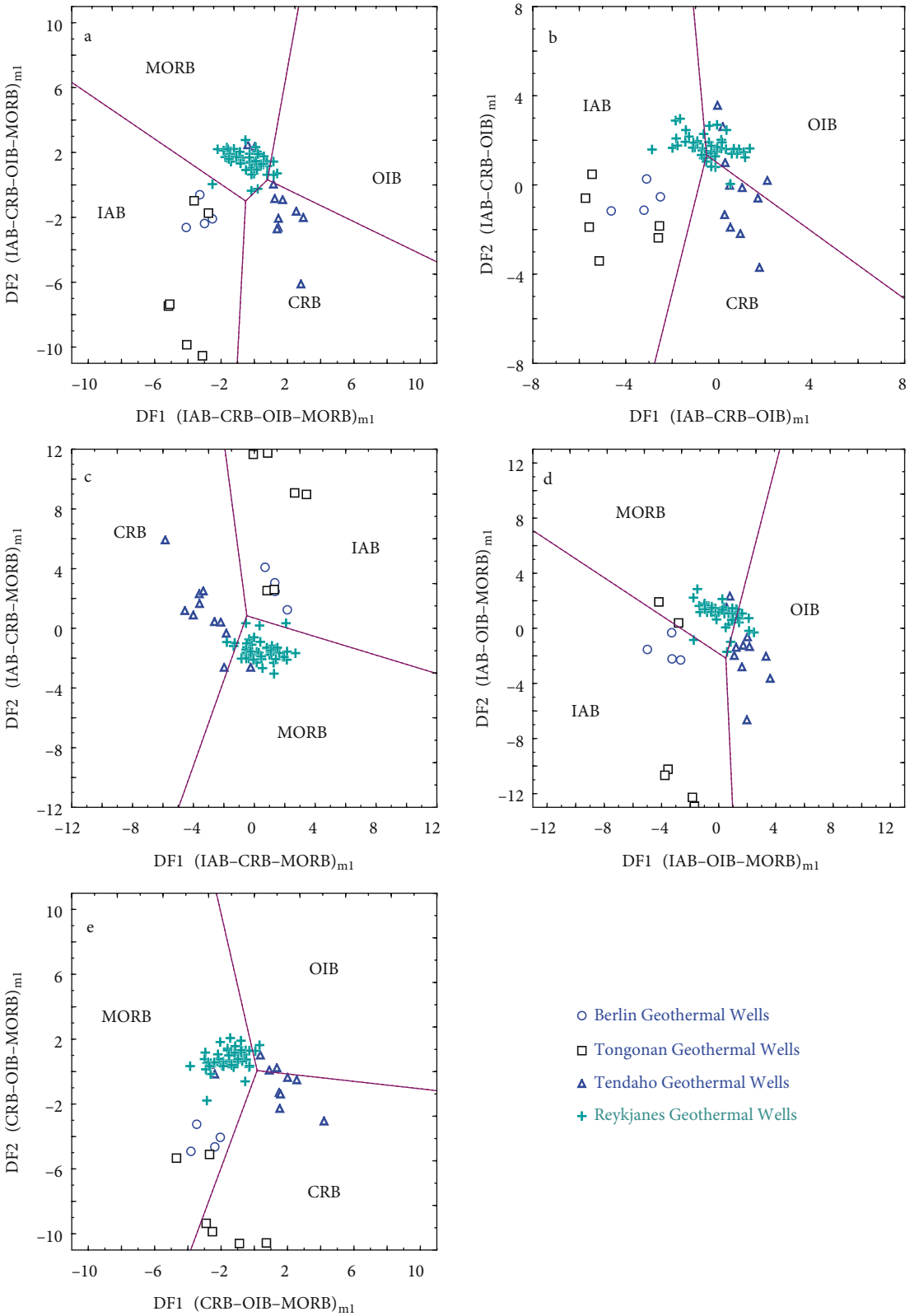

Figure 1. Application of major-element discriminant function-based tectonomagmatic discrimination diagrams of Agrawal et al. (2004) for altered basic rocks of the geothermal wells (see index of the figure for the geothermal wells; IAB: island arc basic rocks, CRB: continental rift basic rocks, OIB: ocean-island basic rocks, MORB: mid-ocean ridge basic rocks).

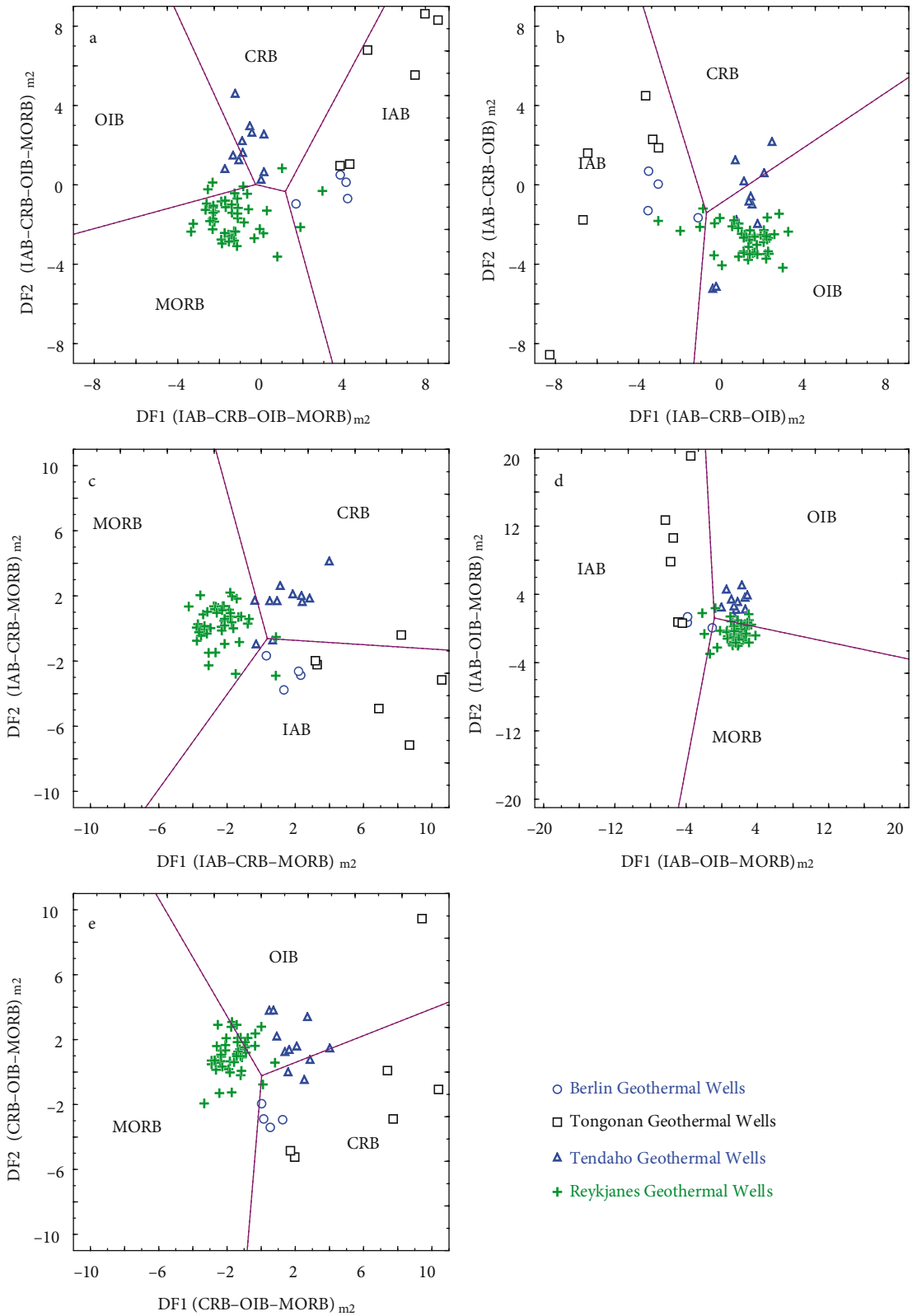

Figure 2. Application of major-element discriminant function-based tectonomagmatic discrimination diagrams of Verma et al. (2006) for altered basic rocks of the geothermal wells (see index of the figure for the geothermal wells; IAB: island arc basic rocks, CRB: continental rift basic rocks, OIB: ocean-island basic rocks, MORB: mid-ocean ridge basic rocks).

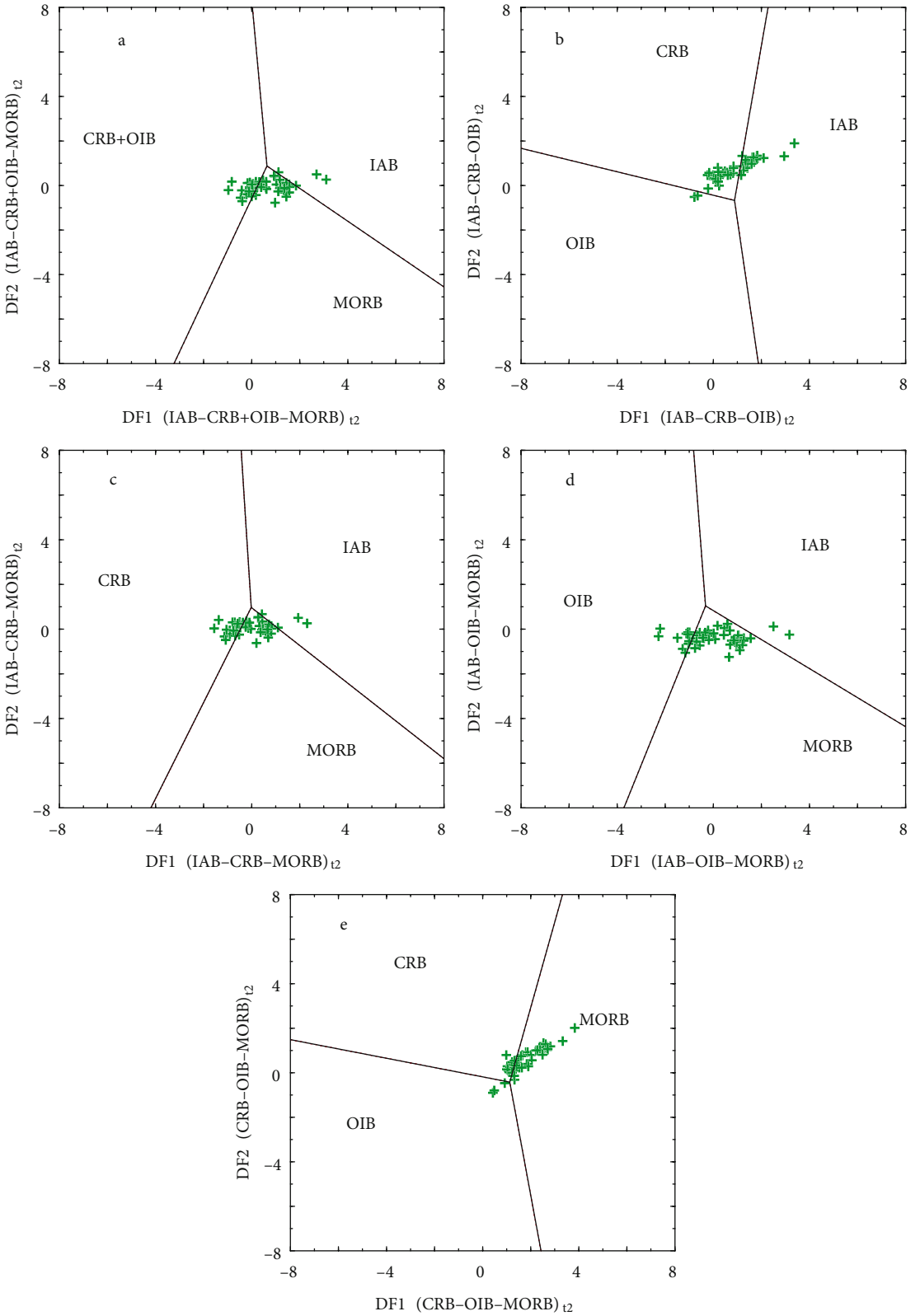

Figure 3. Application of the trace-element discriminant function-based tectonomagmatic discrimination diagrams of Verma and Agrawal (2011) for altered basic rocks of the well from Reykjanes geothermal field, Iceland (IAB: island arc basic rocks, CRB: continental rift, basic rocks OIB: ocean-island basic rocks, MORB: mid-ocean ridge basic rocks).

Table 2. Tectonomagmatic origin obtained for the altered basic rocks from the wells of the geothermal fields by applying major element-based discrimination diagrams of Agrawal et al. (2004). Boldface italic font indicates the inferred tectonic setting for the basic rocks (IAB: island arc basic rocks, CRB: continental rift basic rocks, OIB: ocean-island basic rocks, MORB: mid-ocean ridge basic rocks).

Geothermal field	Discrimination diagram	Total number of samples	Number of discriminated samples (%)			
			IAB (1)	CRB (2)	OIB (3)	MORB (4)
Berlin geothermal field,	1-2-3-4	4	***4***	0	0	0
El Salvador	1-2-3	4	***4***	0	0	---
	1-2-4	4	***4***	0	---	0
	1-3-4	4	***4***	---	0	0
	2-3-4	4	---	0	0	***4***
Reykjanes geothermal field,	1-2-3-4	48	1 (2.1)	0 (0.0)	3 (6.2)	***44 (91.7)***
Iceland	1-2-3	48	20 (41.7)	4 (8.3)	24 (50.0)	---
	1-2-4	48	1 (2.1)	1 (2.1)	---	***46 (95.8)***
	1-3-4	48	1 (2.1)	---	3 (6.2)	***44 (91.7)***
	2-3-4	48	---	0 (0.0)	2 (4.2)	***46 (95.8)***
Tendaho geothermal field,	1-2-3-4	11	0	***9 (81.8)***	0	2 (18.2)
Ethiopia	1-2-3	11	0	***7 (63.6)***	4 (36.4)	---
	1-2-4	11	0	***10 (90.9)***	---	1 (9.1)
	1-3-4	11	0	---	***9 (81.8)***	2 (18.2)
	2-3-4	11	---	***6 2 (54.5)***	***3*** (27.3)	2 (18.2)
Tongonan geothermal field,	1-2-3-4	6	***6***	0	0	0
Philippines	1-2-3	6	***6***	0	0	---
	1-2-4	6	***6***	0	---	0
	1-3-4	6	***6***	---	0	0
	2-3-4	6	---	***4***	0	2

All 4 diagrams of Verma and Verma (2013b) for all 8 intermediate rock samples (100%) have indicated a within-plate (CR+OI) setting (Table 5), whereas the major elements-based discrimination diagrams of Verma et al. (2013) for acid rocks (4 out of 6 samples) have indicated a dominant CA setting followed by an IA setting for these acid rocks (Table 5).

The known tectonic setting of CPGF is CR (extensional setting; Elders et al., 1984). The tectonic setting indicated by the major elements-based diagrams for these altered rocks is consistent with the known tectonic setting of this geothermal field.

4.4. Reykjanes geothermal field, Iceland

The compiled database consists of major and trace element data for 50 hydrothermally altered rock samples (48 basic and 2 intermediate rocks) representing different depths in a well of the Reykjanes geothermal field (Table 1). All 3 sets of 5 diagrams for basic-ultrabasic rocks have clearly shown a dominant MORB setting. The diagrams based on major element ratios (Agrawal et al., 2004; Figure 1), major element log-ratios (Verma et al., 2006; Figure 2) and log-ratios of immobile major and trace elements (Verma and Agrawal, 2011; Figure 3) have indicated, respectively, 91% to 96%, 56% to 94%, and 52% to 71% of the basic rocks representing the dominant MORB setting (Table 2–4). Some of these discrimination diagrams also indicated a less significant OIB setting.

The major element-based discrimination diagrams of Verma and Verma (2013b) for intermediate rocks have shown a combined within plate (CR+OI) and IA setting (Table 5), whereas combined immobile major and trace elements-based discrimination diagrams of Verma and Verma (2013b) have indicated a clear dominant within plate (CR+OI) tectonic setting for these intermediate rocks. The diagrams of intermediate rocks (Verma and Verma, 2013b) discriminate among the IA, CA, within plate (CR+OI), and collision (Col) setting fields but did not contain the MORB setting. Hence, in the absence of the MORB setting field, these diagrams have indicated a dominant within plate (CR+OI) tectonic setting.

The Reykjanes geothermal field, Iceland, lies along the mid-ocean ridge system in the North Atlantic Ocean.

Table 3. Tectonomagmatic origin obtained for the altered basic rocks from the wells of the geothermal fields by applying major element-based discrimination diagrams of Verma et al. (2006). Boldface italic font indicates the inferred tectonic setting for the basic rocks (IAB: island arc basic rocks, CRB: continental rift basic rocks, OIB: ocean-island basic rocks, MORB: mid-ocean ridge basic rocks).

Geothermal field	Discrimination diagram	Total number of samples	Number of discriminated samples (%)			
			IAB (1)	CRB (2)	OIB (3)	MORB (4)
Berlin geothermal field,	1-2-3-4	4	***4***	0	0	0
El Salvador	1-2-3	4	***4***	0	0	---
	1-2-4	4	***4***	0	---	0
	1-3-4	4	***4***	---	0	0
	2-3-4	4	---	4	0	0
Reykjanes geothermal field,	1-2-3-4	48	2 (4.2)	1 (2.1)	3 (6.2)	***42 (87.5)***
Iceland	1-2-3	48	4 (8.3)	0 (0.0)	44 (91.7)	---
	1-2-4	48	2 (4.2)	1 (2.1)	---	***45 (93.8)***
	1-3-4	48	2 (4.2)	---	***19 (39.6)***	***27 (56.2)***
	2-3-4	48	---	1 (2.1)	15 (31.2)	***32 (66.7)***
Tendaho geothermal field,	1-2-3-4	11	0	***8 (72.7)***	3 (27.3)	0
Ethiopia	1-2-3	11	0	4 (36.4)	***7 (63.6)***	---
	1-2-4	11	1	***8 (72.7)***	---	2
	1-3-4	11	0	---	***11 (100.0)***	0
	2-3-4	11	---	4 (36.4)	***8 (72.7)***	0
Tongonan geothermal field,	1-2-3-4	6	***5***	1	0	0
Philippines	1-2-3	6	***6***	0	0	---
	1-2-4	6	***5***	1	---	0
	1-3-4	6	***5***	---	1	0
	2-3-4	6	---	5	1	0

Table 4. Tectonomagmatic origin obtained for the altered basic rocks from the wells of the geothermal fields by applying the discrimination diagrams, based on log-ratios of immobile major and trace elements of Verma and Agrawal (2011). Boldface italic font indicates the inferred tectonic setting for the basic rocks (IAB: island arc basic rocks, CRB: continental rift basic rocks, OIB: ocean-island basic rocks, MORB: mid-ocean ridge basic rocks).

Geothermal field	Discrimination diagram	Total number of samples	Number of discriminated samples (%)				
			IAB (1)	CRB (2)	CRB (2) + OIB (3)	OIB (3)	MORB (4)
Reykjanes geothermal field,	1-2+3-4	48	4 (8.3)	---	18 (37.5)	---	***26 (54.2)***
Iceland	1-2-3	48	22 (45.8)	24 (50.0)	---	2 (4.2)	---
	1-2-4	48	4 (8.3)	19 (39.6)	---	---	***25 (52.1)***
	1-3-4	48	2 (4.2)	---	---	12 (25.0)	***34 (70.8)***
	2-3-4	48	---	11 (22.9)	---	3 (6.2)	***34 (70.8)***

Marks et al. (2010) have reported that the major and trace element data of the drilled well rock cuttings have indicated a transitional MORB to OIB composition. Verma (2013) has applied the discrimination diagrams for deciphering the compositional similarities and differences between Hawaiian and Icelandic volcanism and has also indicated a transitional tectonic setting of ocean island to mid-ocean ridge (OIB-MORB) for the basic magmas of Iceland. Verma (2013) has concluded that the mid-ocean ridge system clearly influences the Icelandic magmas. The inferred tectonic setting for the hydrothermally altered geothermal well rocks of the Reykjanes geothermal field,

Table 5. Tectonomagmatic origin obtained for the altered intermediate rocks of the wells of different geothermal fields based on multidimensional tectonic discrimination diagrams of Verma and Verma (2013b). Boldface italic font indicates the inferred tectonic setting (IA: island arc, CA: Continental arc, CR: continental rift, OI: Ocean Island, Col: Collision).

Geothermal field	Diagrams based on	Type of the discrimination diagram	Total number of samples	Number of discriminated samples (%)				
				Arc			Within-plate	Collision
				IA+CA	IA	CA	CR+OI	Col
Ahuachapán, El Salvador	Major elements	IA+CA-CR+OI-Col	10	***7***	---	---	0	3
		IA-CA-CR+OI	10	---	***8***	2	0	---
		IA-CA-Col	10	---	***7***	2	---	1
		IA-CR+OI-Col	10	---	6	---	0	4
		CA-CR+OI-Col	10	---	---	6	0	4
	Immobile major and trace elements	IA+CA-CR+OI-Col	8	***8***	---	---	0	0
		IA-CA-CR+OI	8	---	***8***	0	0	---
		IA-CA-Col	8	---	***8***	0	---	0
		IA-CR+OI-Col	8	---	8	---	0	0
		CA-CR+OI-Col	8	---	---	8	0	0
Berlin, El Salvador	Major elements	IA+CA-CR+OI-Col	8	***8***	---	---	0	0
		IA-CA-CR+OI	8	---	4	***4***	0	---
		IA-CA-Col	8	---	3	***5***	---	0
		IA-CR+OI-Col	8	---	8	---	0	0
		CA-CR+OI-Col	8	---	---	8	0	0
Cerro Prieto, Mexico	Major elements	IA+CA-CR+OI-Col	8	0	---	---	***8***	0
		IA-CA-CR+OI	8	---	0	0	***8***	---
		IA-CA-Col	8	---	4	4	---	0
		IA-CR+OI-Col	8	---	0	---	***8***	0
		CA-CR+OI-Col	8	---	---	0	***8***	0
Reykjanes, Iceland	Major elements	IA+CA-CR+OI-Col	2	1	---	---	1	0
		IA-CA-CR+OI	2	---	1	0	1	---
		IA-CA-Col	2	---	2	0	---	0
		IA-CR+OI-Col	2	---	1	---	1	0
		CA-CR+OI-Col	2	---	---	1	1	0
	Immobile major and trace elements	IA+CA-CR+OI-Col	2	0	---	---	2	0
		IA-CA-CR+OI	2	---	0	0	2	---
		IA-CA-Col	2	---	1	1	---	0
		IA-CR+OI-Col	2	---	0	---	2	0
		CA-CR+OI-Col	2	---	---	0	2	0
Roman volcanic provenance	Major elements	IA+CA-CR+OI-Col	4	1	---	---	0	3
		IA-CA-CR+OI	4	---	4	0	0	---
		IA-CA-Col	4	---	2	0	---	2
		IA-CR+OI-Col	4	---	2	---	0	2
		CA-CR+OI-Col	4	---	---	1	0	3
	Immobile major and trace elements	IA+CA-CR+OI-Col	4	2	---	---	0	2
		IA-CA-CR+OI	4	---	4	0	0	---
		IA-CA-Col	4	---	3	0	---	1

Table 5. (continued).

		IA-CR+OI-Col	4	---	3	---		0	1
		CA-CR+OI-Col	4	---	---	0	0		4
Tendaho,	Major elements	IA+CA-CR+OI-Col	1	0	---	---	1		0
Ethiopia		IA-CA-CR+OI	1	---	0	0	1		---
		IA-CA-Col	1	---	0	0	---		1
		IA-CR+OI-Col	1	---	0	---		1	0
		CA-CR+OI-Col	1	---	---	0	1		0
Tongonan,	Major elements	IA+CA-CR+OI-Col	4	1	---	---	0		3
Philippines		IA-CA-CR+OI	4	---	1	2	1		---
		IA-CA-Col	4	---	0	1	---		3
		IA-CR+OI-Col	4	---	2	---		0	2
		CA-CR+OI-Col	4	---	---	2	0		2

Table 6. Tectonomagmatic origin obtained for the acid rocks of the wells of different geothermal fields based on multidimensional tectonic discrimination diagrams of Verma et al. (2013). Boldface italic font indicates the inferred tectonic setting (IA: island arc, CA: Continental arc, CR: continental rift, OI: Ocean Island, Col: Collision).

Geothermal field	Diagrams based on	Type of the discrimination diagram	Total number of samples	Number of discriminated samples (%)					
				Arc			Within-plate		Collision
				IA+CA	IA	CA	CR+OI		Col
Ahuachapán,	Major elements	IA+CA-CR+OI-Col	4	4	---	---	0		0
El Salvador		IA-CA-CR+OI	4	---	4	0	0		---
		IA-CA-Col	4	---	2	0	---		2
		IA-CR+OI-Col	4	---	4	---		0	0
		CA-CR+OI-Col	4	---	---	4	0		0
	Immobile major	IA+CA-CR+OI-Col	3	3	---	---	0		0
	and trace	IA-CA-CR+OI	3	---	1	2	0		---
	elements	IA-CA-Col	3	---	1	2	---		0
		IA-CR+OI-Col	3	---	3	---		0	0
		CA-CR+OI-Col	3	---	---	3	0		0
Cerro Prieto,	Major elements	IA+CA-CR+OI-Col	6	6	---	---	0		0
Mexico		IA-CA-CR+OI	6	---	2	***4***	0		---
		IA-CA-Col	6	---	2	***4***	---		0
		IA-CR+OI-Col	6	---	6	---		0	0
		CA-CR+OI-Col	6	---	---	6	0		0

Iceland, in the present study is the dominant MORB setting followed by within plate (CR+OI) setting and is therefore consistent with the known tectonic setting for this geothermal field.

4.5. Roman Volcanic Province, Italy

The compiled database consists of major and trace element data for 4 hydrothermally altered intermediate rock samples obtained from 4 wells (1 rock sample from each well) of the Roman Volcanic Province (Table 1). The major element-based diagrams for the intermediate rocks (Verma and Verma, 2013b) have suggested IA and collision (Col) settings (Table 5). The combined immobile major and trace element-based discrimination diagrams of Verma and Verma (2013b) for these rocks have also suggested a dominant IA setting (Table 5).

Magma genesis and tectonic setting of the volcanism in the Roman Province was a subject of controversy between subduction beneath the Calabrian Arc (Edgar,

1980) or related to a continental rift (Cundari, 1980). It is also reported that their geochemical compositions are different to those of continental rift lavas but similar to those of island arcs (Thompson, 1977; Foden and Varne, 1980; Ewart, 1982). The inferred dominant IA tectonic setting by the major and the combined immobile major and trace element-based discrimination diagrams (Verma and Verma, 2013b) in the present work also suggests that the geochemical compositions of these intermediate rocks are different to those of continental rift lavas (none of the samples have indicated the CR+OI setting) but similar to those of island arcs.

4.6. Tendaho geothermal field, Afar region

The compiled database consists of only the major element data for 12 hydrothermally altered rock samples (7 basic, 4 ultrabasic, and 1 intermediate) representing different depths in 3 wells of the Tendaho geothermal field.

The major element-based discrimination diagrams (Agrawal et al., 2004; Figure 1) have indicated a clear dominant CRB setting (63.6%–90.9%; Table 2), whereas major elements log-ratios-based discrimination diagrams of Verma et al. (2006) (Figure 2) have indicated CRB (36%–73%) and OIB (27%–73%) settings for these rocks (Table 2).

The major elements-based discrimination diagrams of Verma and Verma (2013b) have also indicated a within plate (CR+OI) setting for the only available intermediate rock.

The Tendaho geothermal field lies in the Afar region in a 50-km-wide rift, considered to be the southern extension, on land, of the Red Sea structure joining the Ethiopian Rift (Gianelli et al., 1998). Therefore, the rift tectonic setting inferred from these discrimination diagrams is consistent with the known tectonic setting of the region.

4.7. Tongonan geothermal field, Philippines

The compiled database consists of only the major element data for 10 hydrothermally altered rock samples (6 basic and 4 intermediate rocks) representing different depths in 8 wells of the Tongonan geothermal field (Table 1).

Two sets of major element-based discrimination diagrams (Agrawal et al., 2004; Verma et al., 2006) for basic rocks have indicated a very clear IAB setting (100%; Tables 2 and 3; Figures 1 and 2), whereas the major elements-based discrimination diagrams of Verma and Verma (2013b) for intermediate rocks have shown a dominant collision tectonic setting.

The Tongonan geothermal field is located in the Philippine archipelago and hence the known tectonic setting of this geothermal field is IA. The tectonic setting inferred by the discrimination by basic rocks (Agrawal et al., 2004; Verma et al., 2006) is consistent with the known tectonic setting of the region.

5. Overall performance of the multielement discriminant function-based diagrams

Overall performances of the more recently developed multielement discriminant function-based diagrams for basic (Agrawal et al., 2004; Verma et al., 2006; Agrawal et al., 2008; Verma and Agrawal, 2011), intermediate (Verma and Verma, 2013b), and acid rocks (Verma et al., 2013) in inferring the original tectonic setting of the hydrothermally altered geothermal well rocks are as follows: (1) all the applied tectonic discrimination diagrams have inferred tectonic settings consistent, in general, with the known tectonic setting for 5 out of the 7 studied geothermal fields (Berlin geothermal field, El Salvador; Cerro Prieto geothermal field, Mexico; Reykjanes geothermal field, Iceland; Tendaho geothermal field, Afar region; and Roman volcanic provenance, Italy); (2) only the tectonic discrimination diagrams of the basic rocks have inferred the correct tectonic setting for the Tongonan geothermal field; and (3) the diagrams based on combination of immobile major and trace elements for acid rocks have indicated the correct tectonic setting for the well rocks of the Ahuachapán geothermal field, El Salvador.

6. Conclusions

The present study suggests that hydrothermal alteration-induced chemical changes in volcanic rocks may not significantly affect the application of the recently developed and highly successful multielement discriminant function-based diagrams for basic (Agrawal et al., 2004, 2008; Verma et al., 2006; Verma and Agrawal, 2011), intermediate (Verma and Verma, 2013b), and acid rocks (Verma et al., 2013). These diagrams, in general, successfully inferred the tectonomagmatic origin of the hydrothermally altered volcanic rocks in the drilled wells of the important geothermal fields of the world. This confirms the robustness of these diagrams in inferring the tectonomagmatic origin of igneous rocks.

Acknowledgment

This work was partly supported by UNAM-PAPIIT project IN104813.

References

Agrawal S, Verma SP (2007). Comment on 'Tectonic classification of basalts with classification trees' by Pieter Vermeesch (2006). Geochim Cosmochim AC 71: 3388–3390.

Agrawal S, Guevara M, Verma SP (2004). Discriminant analysis applied to establish major-element field boundaries for tectonic varieties of basic rocks. Int Geol Rev 46: 575–594.

Agrawal S, Guevara M, Verma SP (2008). Tectonic discrimination of basic and ultrabasic rocks through log-transformed ratios of immobile trace elements. Int Geol Rev 50: 1057–1079.

Agostini S, Corti G, Doglioni C, Carminati E, Innocenti F, Tonarini S, Manetti P, Di Vincenzo G, Montanari D (2006). Tectonic and magmatic evolution of the active volcanic front in El Salvador: insight into the Berlín and Ahuachapán geothermal areas. Geothermics 35: 368–408.

Barnett V, Lewis T (1994). Outliers in Statistical Data. 3rd ed. Chichester, UK: Wiley.

Beccaluva L, Di Girolamo P, Serri G (1991). Petrogenesis and tectonic setting of the Roman Volcanic Province, Italy. Lithos 26: 191–221.

Butler JC, Woronow A (1986). Discrimination among tectonic settings using trace element abundances of basalts. J Geophys Res 91: 10289–10300.

Cabanis B, Lecolle M (1989). Le diagramme La/10-Y/15-Nb/8: un outil pour la discrimination des séries volcaniques et la mise en évidence des processus de mélange et/ou de contamination crustale. CR Acad Sci Paris 309: 2023–2029 (in French).

Cundari A (1980). Role of subduction in the genesis of leucite-bearing rocks: Facts on fashion? Contrib Mineral Petrol 73: 432–434.

De Groot P, Baker JH (1992). High element mobility in 1.9–1.86 Ga hydrothermal alteration zones, Bergslagen, central Sweden: relationships with exhalative Fe-ore mineralizations. Precambrian Res 54: 109–130.

Dickin AP (1981). Hydrothermal leaching of rhyolite glass in the environment has implications for nuclear waste disposal. Nature 294: 342–347.

Edgar AD (1980). Role of subduction of the genesis of leucite-bearing rocks: discussion. Contrib Mineral Petrol 73: 429–431.

Elders WA, Bird DK, Williams AE, Schiffmann P (1984). Hydrothermal flow regime and magmatic heat source of the Cerro Prieto geothermal system, Baja California, Mexico. Geothermics 13: 27–47.

Ewart A (1982). The mineralogy and petrology of Tertiary-Recent orogenic volcanic rocks: with special reference to the andesitic-basaltic compositional range. In: Thorpe RS, editor, Andesites. Chichester, UK: Wiley, pp. 25–98.

Finlow-Bates T, Stumpfl EF (1981). The behaviour of so-called immobile elements in hydrothermally altered rocks associated with volcanogenic submarine-exhalative ore deposits: Miner Deposita 16: 319–328.

Floyd PA, Winchester JA (1975). Magma type and tectonic setting discrimination using immobile elements. Earth Planet Sc Lett 27: 211–218.

Foden JD, Varne R (1980). The petrology and tectonic setting of Quaternary-recent volcanic centres of Lombok and Sumbawa, Sunda Arc. Chem Geol 30: 201–226.

Gianelli G, Mekuria N, Battaglia S, Chersicla A, Garofalo P, Ruggieri G, Manganelli M, Gebregziabher Z (1998). Water–rock interaction and hydrothermal mineral equilibria in the Tendaho geothermal system. J Volcanol Geoth Res 86: 253–276.

Herzig CT (1990). Geochemistry of igneous rocks from the Cerro Prieto geothermal field, northern Baja California, Mexico. J Volcanol Geoth Res 42: 261–271.

Humphris SE, Thompson G (1978). Trace element mobility during hydrothermal alteration of oceanic basalts. Geochim Cosmochim AC 42: 127–136.

Kelepertsis AE, Esson J (1987). Major- and trace-element mobility in altered volcanic rocks near Stypsi, Lesbos, Greece and genesis of a kaolin deposit. Appl Clay Sci 2: 11–28.

Kuschel E, Smith IE (1992). Rare earth mobility in young arc-type volcanic rocks from northern New Zealand: Geochim Cosmochim AC 56: 3951–3955.

Marks N, Schiffman P, Zierenberg RA, Franzson H, Fridleifsson GÓ (2010). Hydrothermal alteration in the Reykjanes geothermal system: insights from Iceland deep drilling program well RN-17. J Volcanol Geoth Res 189: 172–190.

Meschede M (1986). A method of discriminating between different types of mid-ocean ridge basalts and continental tholeiites with the Nb-Zr-Y diagram. Chem Geol 56: 207–218.

Mullen ED (1983). $MnO/TiO_2/P_2O_5$: a minor element discrimination for basaltic rocks of oceanic environments and its implications for petrogenesis. Earth Planet Sc Lett 62: 53–62.

Nicholson K (1993). Geothermal Fluids: Chemistry and Exploration Techniques. Berlin, Germany: Springer-Verlag.

Palacios CM, Hein UF, Dulski P (1986). Behavior of rare earth elements during hydrothermal alteration at the Buena Esperanza copper–silver deposit, northern Chile. Earth Planet Sc Lett 80: 208–216.

Pandarinath K, Dulski P, Torres-Alvarado IS, Verma SP (2008). Element mobility during the hydrothermal alteration of rhyolitic rocks of the Los Azufres geothermal field, Mexico. Geothermics 37: 53–72.

Pandarinath K, Verma SK (2013). Application of four sets of tectonomagmatic discriminant function based diagrams to basic rocks from northwest Mexico. J Iber Geol 39: 181–195.

Pearce JA (1976). Statistical analysis of major element patterns in basalts. J Petrol 17: 15–43.

Pearce JA (1982). Trace element characteristics of lavas from destructive plate boundaries: In: Thorpe RS, editor. Andesites. Chichester, UK: Wiley.

Pearce JA, Cann JR (1973). Tectonic setting of basic volcanic rocks determined using trace element analyses. Earth Planet Sc Lett 19: 290–300.

Pearce JA, Gale GH (1977). Identification of ore-deposition environment from trace-element geochemistry of associated igneous host rocks: Geological Society of London Special Publication 7: 14–24.

Pearce TH, Gorman BE, Birkett TC (1977). The relationship between major element chemistry and tectonic environment of basic and intermediate volcanic rocks. Earth Planet Sc Lett 36: 121–132.

Pearce A, Norry MJ (1979). Petrogenetic implications of Ti, Zr, Y, and Nb variations in volcanic rocks. Contrib Mineral Petr 69: 33–47.

Rubin JN, Henry CD, Price JG (1993). The mobility of zirconium and other "immobile" elements during hydrothermal alteration. Chem Geol 110: 29–47.

Ruggieri G, Petrone CM, Gianelli G, Arias A, Henriquez ET (2006). Hydrothermal alteration in the Berlin geothermal field (El Salvador): new data and discussion on the natural state of the system. Period Mineral 75: 293–312.

Scott G (2004). Major active faults determine the location of the Tongonan geothermal field: Evidence provided by rock alteration and stable isotope geochemistry. Isl Arc 13: 370–386.

Shervais JW (1982). Ti-V plots and the petrogenesis of modern and ophiolitic lavas. Earth Planet Sc Lett 59: 101–118.

Sheth HC (2008). Do major oxide tectonic discrimination diagrams work? Evaluating new log-ratio and discriminant-analysis-based diagrams with Indian Ocean mafic volcanics and Asian ophiolites. Terra Nova 20: 229–236.

Sturchio NC, Muehlenbachs K, Seitz M (1986). Element redistribution during hydrothermal alteration of rhyolite in an active geothermal system: Yellowstone drill cores Y-7 and Y-8. Geochim Cosmochim AC 50: 1619–1631.

Thompson RN (1977). Primary basalts and magma genesis. III. Alban Hills, Roman Comagmatic Province, Central Italy. Contrib Mineral Petrol 60: 91–108.

Vasconcelos-F M, Verma SP, Rodríguez-G, JF (1998). Discriminación tectónica: nuevo diagrama Nb-Ba para arcos continentales, arcos insulares, "rifts" e islas oceánicas en rocas máficas. Boletín de la Sociedad Española de Mineralogía 21: 129–146 (in Spanish).

Vasconcelos-F M, Verma SP, Vargas-B RC (2001). Diagrama Ti-V: una nueva propuesta de discriminación para magmas básicos en cinco ambientes tectónicos. Rev Mex Cienc Geol 18: 162-174 (in Spanish).

Verma SK, Oliveira EP (2013). Application of multi-dimensional discrimination diagrams and probability calculations to Paleoproterozoic acid rocks from Brazilian cratons and provinces to infer tectonic settings. J S Am Earth Sci 45: 117–146.

Verma SK, Pandarinath K, Verma SP (2012). Statistical evaluation of tectonomagmatic discrimination diagrams for granitic rocks and proposal of new discriminant-function-based multi-dimensional diagrams for acid rocks. Int Geol Rev 54: 325–347.

Verma SK, Verma SP (2013a). Identification of Archaean plate tectonic processes from multidimensional discrimination diagrams and probability calculations. Int Geol Rev 55: 225–248.

Verma SP (1997). Sixteen statistical tests for outlier detection and rejection in evaluation of International Geochemical Reference Materials: example of microgabbro PM-S. Geostandard Newslett 21: 59–75.

Verma SP (2010). Statistical evaluation of bivariate, ternary and discriminant function tectonomagmatic discrimination diagrams. Turkish J Earth Sci 19: 185–238.

Verma SP (2013). Application of 50 multi-dimensional discrimination diagrams and significance tests: deciphering compositional similarities and differences between Hawaiian and Icelandic volcanism. Int Geol Rev 55: 1553–1572.

Verma SP, Agrawal S (2011). New tectonic discrimination diagrams for basic and ultrabasic volcanic rocks through log-transformed ratios of high field strength elements and implications for petrogenetic processes. Rev Mex Cienc Geol 28: 24–44.

Verma SP, Díaz-González L (2012). Application of the discordant outlier detection and separation system in geosciences. Int Geol Rev 54: 593–614.

Verma SP, Guevara M, Agrawal S (2006). Discriminating four tectonic settings: five new geochemical diagrams for basic and ultrabasic volcanic rocks based on log-ratio transformation of major-element data. J Earth Syst Sci 115: 485–528.

Verma SP, Pandarinath K, Verma SK, Agrawal S (2013). Fifteen new discriminant-function-based multi-dimensional robust diagrams for acid rocks and application to Precambrian rocks. Lithos 168-169: 113–123.

Verma SP, Quiroz-Ruiz A (2006a). Critical values for six Dixon tests for outliers in normal samples up to sizes 100, and applications in science and engineering. Rev Mex Cienc Geol 23: 133–161.

Verma SP, Quiroz-Ruiz A (2006b). Critical values for 22 discordancy test variants for outliers in normal samples up to sizes 100, and applications in science and engineering. Rev Mex Cienc Geol 23: 302–319.

Verma SP, Quiroz-Ruiz A (2008). Critical values for 33 discordancy test variants for outliers in normal samples for very large sizes of 1,000 to 30,000. Rev Mex Cienc Geol 25: 369–381.

Verma SP, Quiroz-Ruiz A, Díaz-González L (2008). Critical values for 33 discordancy test variants for outliers in normal samples up to sizes 1000, and applications in quality control in Earth Sciences. Rev Mex Cienc Geol 25: 82–96.

Verma SP, Quiroz-Ruiz A (2010). Corrigendum to ´Critical values for 22 discordancy test variants for outliers in normal samples up to sizes 100, and applications in science and engineering [Rev. Mex. Cienc. Geol., 23 (2006), 302-319]´. Rev Mex Cienc Geol 25: 202.

Verma SP, Rivera-Gómez MA (2013). New computer program TecD for tectonomagmatic discrimination from discriminant function diagrams for basic and ultrabasic magmas and its application to ancient rocks. In: Verma SP, Pandarinath K, editors. Monograph on Geochemistry in Mexico. J Iber Geol 39: 167–179.

Verma SP, Rodríguez-Ríos R, González-Ramírez R (2010). Statistical evaluation of classification diagrams for altered igneous rocks. Turkish J Earth Sci 19: 239–265.

Verma SP, Torres-Alvarado IS, Satir M, Dobson PF (2005). Hydrothermal alteration effects in geochemistry and Sr, Nd, Pb, and O isotopes of magmas from the Los Azufres geothermal field (Mexico): a statistical approach. Geochem J 39: 141–163.

Verma SP, Torres-Alvarado IS, Sotelo-Rodríguez ZT (2002). SINCLAS: standard igneous norm and volcanic rock classification system. Comput Geosci 28: 711–715.

Verma SP, Torres-Alvarado IS, Velasco-Tapia F (2003). A revised CIPW norm. Schweiz Miner Petrog 83: 197–216.

Verma SP, Verma SK, Pandarinath K, Rivera-Gómez MA (2011). Evaluation of recent tectonomagmatic discrimnation diagrams and their application to the origin of basic magmas in Southern Mexico and Central America. Pure Appl Geophys 168: 1501–1525.

Verma SP, Verma SK (2013b). First 15 probability-based multidimensional tectonic discrimination diagrams for intermediate magmas and their robustness against postemplacement compositional changes and petrogenetic processes. Turkish J Earth Sci 22: 931–995.

Vermeesch P (2006). Tectonic discrimination of basalts with classification trees: Geochim Cosmochim AC 70: 1839–1848.

Wood DA (1980). The application of a Th-Hf-Ta diagram to problems of tectonomagmatic classification and to establishing the nature of crustal contamination of basaltic lavas of the British Tertiary volcanic province. Earth Planet Sc Lett 50: 11–30.